Thermochimica Acta 511 (2010) 168–173

Contents lists available at ScienceDirect

Thermochimica Acta

journal homepage: www.elsevier.com/locate/tca

# Comparison of thermal property and dissolution behavior of synthetic compound and natural hemimorphite

Zhiying Ding, Zhoulan Yin*, Huiping Hu, Qiyuan Chen

*College of Chemistry and Chemical Engineering, Central South University, Hunan 410083, China*

ARTICLE INFO

*Article history:*
Received 7 May 2010
Received in revised form 4 August 2010
Accepted 9 August 2010
Available online 14 August 2010

*Keywords:*
Thermal property
Hemimorphite
Synthesis
Dissolution
Ammoniacal solution

ABSTRACT

A comparison of the thermodynamic properties, crystal structure, thermal characterization and dissolution behavior of the synthetic compound and the natural hemimorphite was made. It was found that the synthetic compound shows the same crystal structure but is poorly crystallized compared with the natural hemimorphite. Both the synthetic compound and natural hemimorphite display the similar characteristics of phase formation during calcination, except that the poor crystallization of synthetic compound leads to the structural reorganization with an intense exothermic peak at 700 °C to form a stable phase after losing structural water at 633 °C. The natural hemimorphite exhibits an endothermic peak at 700 °C for the removal of structural water during TGA/DTA analysis. Although, synthetic compound shows a more rapid dissolution rate than the natural hemimorphite in ammoniacal solution, the final states exhibit the same when they are completely dissolved.



## 1. Introduction

Hemimorphite, $Zn_4Si_2O_7(OH)_2{\cdot}H_2O$, belongs to the orthorhombic system, space group Imm2. The crystal structure of hemimorphite has been determined by Ito and West [1], Bahclay and Cox [2], Mcdonald and Cruickshank [3], Hill and Gibbs [4] and Libowitzky and Schultz [5]. It was described as consisting of three membered rings of corner-sharing $Zn(OH)O_3$ and $SiO_4$ tetrahedra arranged in compact sheets parallel to (0 1 0) (Fig. 1a). Three oxygen atoms in each tetrahedron are bonded to two zinc atoms and one silicon atom, while a fourth oxygen atom forms a bridging bond to an equivalent cation in an adjacent sheet. The cross-bridging of the sheets produces additional rings of four, six and eight tetrahedra and forms a series of large cavities connected along the *c*-axis (Fig. 1b).

According to the literature [6], there are independent water molecules (crystallization water) and the OH groups in the crystal of hemimorphite. On heating, it is apparent that $H_2O$ molecule is able to pass through the six-membered ring into the adjacent (vacated) cavity above or below the *c*-axis without disruption of the structure. Upon heating, crystallization water is continuously lost between 393 and 657 °C, whereas loss of hydroxyl groups and breakdown of the structure occur at 740 °C. Above 740 °C, anhydrous β-$Zn_2SiO_4$ is formed which will transform into willemite at 960 °C. The phase characteristics of these high-temperature products on heating were investigated [7]. Hydrothermal experiments [8] showed that hemimorphite is stable under ~250 °C at 2–3 kbar, above which willemite is stable. There is a contraction of the structure and the channels upon expulsion of the water molecules. The mechanism of structural contraction is dependent upon the collapse of the cavities interconnected parallel to *c*-axis towards the expelled water molecules.

Hemimorphite is widely used as jewel for its nice appearance and high hardness. Meanwhile, hemimorphite is an important raw material for zinc extraction. As a secondary mineral typically found in the oxidized zone of zinc-bearing mineral deposits, hemimorphite is hardly separated from the zinc-oxidized ores in various carbonates and silicates, such as smithsonite ($ZnCO_3$), hydrozincite ($Zn_5(CO_3)_2(OH)_6$), zincite (ZnO), willemite ($Zn_2SiO_4$) and so on [9,10]. Since ammonia leaching has been given more attention in treating low grade complex zinc ores [11], and hydrometallurgical studies show that hemimorphite is relatively difficult to be extracted [12], the studies on the solubility and kinetic behaviors of hemimorphite in ammoniacal solution is important for the hydrometallurgical process of zinc.

Since the natural hemimorphite with high purity is scarce for the thermodynamic study in ammoniacal solutions, the synthetic compound, which has the same chemical formula and composition as the natural hemimorphite, would be of great help if its thermal behavior agrees with the natural hemimorphite. The objective of this research is to compare the thermodynamic properties, crystal structure, thermal characterization and dissolution behavior of the synthetic compound and the natural hemimorphite in ammoniacal solutions.

* Corresponding author. Tel.: +86 731 88877364; fax: +86 731 88879616.
*E-mail addresses:* yzllxh@gmail.com, zhiyingding@gmail.com (Z. Yin).

0040-6031/$ – see front matter © 2010 Elsevier B.V. All rights reserved.
doi:10.1016/j.tca.2010.08.010

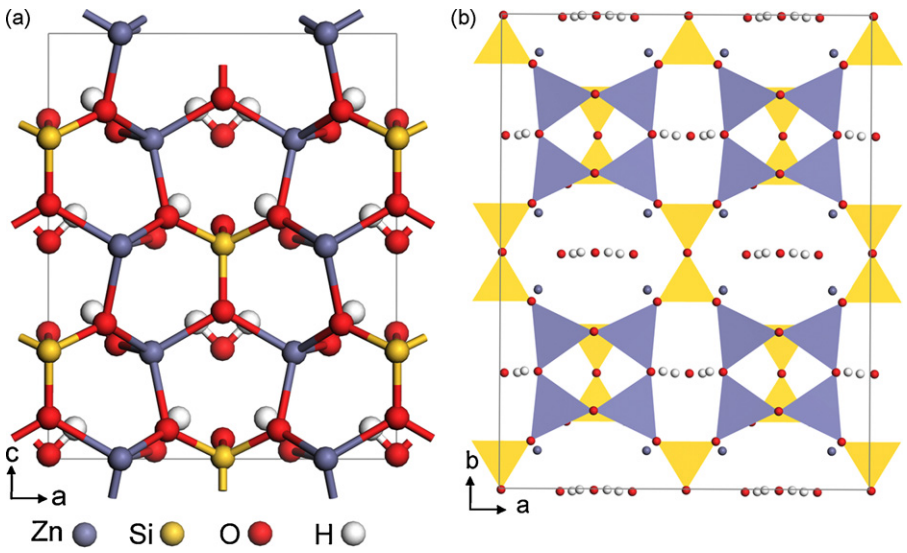


**Fig. 1.** Hemimorphite structure projected in: (a) the (0 1 0) plane; (b) the (0 0 1) plane.

## 2. Experimental

### 2.1. Samples of natural hemimorphite

Samples of natural hemimorphite were obtained from Jinding, Yunnan province in China. The hemimorphite always exhibits slabs, stalactitic, botryoidal and crested masses. The color of massive hemimorphite varies from colorless to white, very light yellow, and light blue. The luster is vitreous and subpearly. Liu et al. [13] studied the color genesis of the hemimorphite and concluded that the blue color might be caused by the partial substitution of $Cu^{2+}$ for $Zn^{2+}$ and the luster was associated with the crystallization water.

### 2.2. Samples of synthetic compound

Synthetic compound, which has the same formula and composition as the natural hemimorphite, was prepared by homogeneous deposition–precipitation method [14]. Aerosil silica (named WACKER HDK T40 with specific surface area of $400 \pm 40\,m^2\,g^{-1}$) suspension in water and appropriate amounts of zinc nitrate hexahydrate (molar ration: Zn/Si = 2) together with urea were heated to 90 °C and kept at the temperature for 30 h. The hydrolysis of urea results in a homogenous pH-rise to make hemimorphite precipitate. After cooling, the precipitate was filtered, washed and dried at 130 °C for 20 h.

### 2.3. Characterization techniques

X-ray diffraction (XRD) studies were performed using Rigaku D/max 2550VB+18 kw powder diffractometer with a Cu/Kα X-ray source at 40 kV and 300 mA. The XRD patterns were recorded with a scan rate of $0.075^\circ\,s^{-1}$ and a sampling interval of 0.02°.

The Nicolet 6700 FTIR spectrometer was employed to record the spectra using the KBr pellet method. Spectra over the 4000–400 $cm^{-1}$ range were obtained with a resolution of 4.00 $cm^{-1}$ and a mirror velocity of 0.6329 cm $s^{-1}$.

The surface morphology of the samples was examined by SEM analysis using Jeol JSM-6360 instrument at 20 kV. The grains mounted on a stub were coated with Au/Pd for observation.

The TGA/DTA analysis was performed on a thermogravimetric analyzer of Universal V4.0C TA instrument with SDT Q600 V8.0 Build 95 in a nitrogen flow of 100 ml $min^{-1}$ and a heating rate of 10 °C $min^{-1}$.

### 2.4. Dissolution experiment

The dissolution experiment was carried out in a round-bottomed split flask, equipped with an efficient stirrer, a mercury thermometer, and a delivery tube for ammoniacal solutions. Temperature control of the flask contents to within ±0.5 °C was achieved with a thermostat controlled by electric heating mantle. 4 g samples of less than 0.075 mm were added into 200 ml solution with 1 mol $L^{-1}$ $NH_3$ and 2 mol $L^{-1}$ $NH_4Cl$ at 25 ± 0.5 °C which was then stirred for some time. 5 ml samples of solution were accurately measured and withdraw periodically for analysis. The zinc concentrations were determined by EDTA titration.

After attainment of equilibrium, the concentration of total ammonia ($NH_3$:$NH_4Cl$ = 1:2, molar ratio) in solution was increased to ensure that samples were dissolved completely. Then, the residues were separated by centrifugation, washed with dilute ammoniacal solution of pH = 9.0 and dried in an oven at 60 °C.

## 3. Results and discussion

### 3.1. XRD and SEM analysis

Figs. 2 and 3, curve 1 show the X-ray diffraction (XRD) patterns of the natural hemimorphite and synthetic compound, respectively. Comparing the XRD patterns to the JCPDS files, it illustrates that all the peaks of the samples are identified as hemimorphite (JCPDS card, No. 85-1387). The composition of natural hemimorphite and synthetic compound is presented in Table 1. It is clear that the natural hemimorphite has a closer composition to the theoretical one than that of the synthetic compound, with up to 98.22% of hemimorphite by Mineralogical analysis. Its morphology appears compact, well-crystallized (as shown in Fig. 4a). In the synthetic compound, the crystallinity is inferior to that of the natural sample, since the XRD background is rougher and the full widths at half maxima (FWHM) are larger than those of the natural hemimorphite. Meanwhile, the morphology is loose and the compound is relatively poorly crystallized (as shown in Fig. 4b). There are two possible factors involved: first, the amount of water is higher than that of the theoretical one, due to the presence of a certain amount of adsorbed water, which is logically considered as the method of preparation of the compound and its lower crystallinity. Second, the

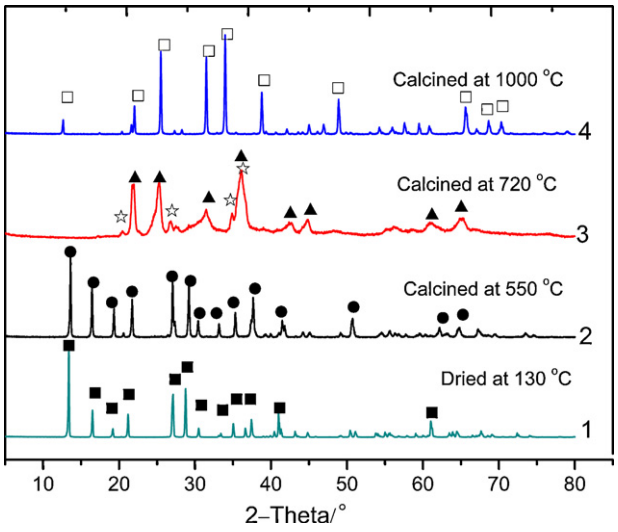


**Fig. 2.** XRD patterns of natural hemimorphite calcined at different temperature. (■) $Zn_4Si_2O_7(OH)_2{\cdot}H_2O$, (●) $Zn_4Si_2O_7(OH)_2$, (☆) $Mg_{0.26}Fe_{1.74}(SiO_4)$, (▲) $Zn_2SiO_4$, (□) willemite. *Note:* 1 – Hemimorphite, orthorhombic, cell = 0.8374 × 1.0719 × 0.5118, vol = 0.4593 nm$^3$. 2 – Hemimorphite, orthorhombic, cell = 0.8382 × 1.0730 × 0.5096, vol = 0.4583 nm$^3$. 3 – $Zn_2SiO_4$, orthorhombic, cell = 0.4792 × 1.0467 × 0.6082, vol = 0.3050 nm$^3$. 4 – Willemite, R-3 (148) (hexagonal), cell = 1.3945 × 0.9317, vol = 1.5692 nm$^3$.

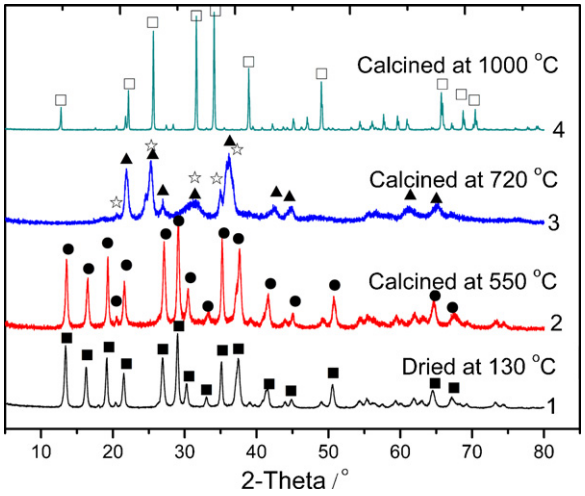


**Fig. 3.** XRD patterns of synthetic compound calcined at different temperature. (■) $Zn_4Si_2O_7(OH)_2{\cdot}H_2O$, (●) $Zn_4Si_2O_7(OH)_2$, (☆) $Mg_{0.26}Fe_{1.74}(SiO_4)$, (▲) $Zn_2SiO_4$, (□) willemite. *Note:* 1 – Hemimorphite, orthorhombic, cell = 0.8376 × 1.0679 × 0.5111, vol = 0.4572 nm$^3$. 2 – Hemimorphite, orthorhombic, cell = 0.8250 × 1.0761 × 0.5096, vol = 0.4525 nm$^3$. 3 – $Zn_2SiO_4$, orthorhombic, cell =0.4768 × 1.0286 × 0.6057, vol = 0.2970 nm$^3$. 4 – Willemite, R-3 (148) (hexagonal), cell = 1.3921 × 0.9298, vol = 1.5605 nm$^3$.

content of $SiO_2$ is higher than that of the theoretical value, probably due to the precipitation of a small amount of amorphous silica. Consequently, the amount of Zn is lower than that of the theoretical one.

**Table 1**
Chemical composition of hemimorphite (%).

| | ZnO | $SiO_2$ | $H_2O$ | $T_{Zn}$ |
|---|---|---|---|---|
| Theoretical composition | 67.58 | 24.94 | 7.48 | 54.29 |
| Natural hemimorphite | 66.41 | 23.14 | 8.70 | 53.35 |
| Synthetic compound | 63.23 | 26.72 | 10.05 | 50.80 |

$T_{Zn}$: total zinc content of samples.

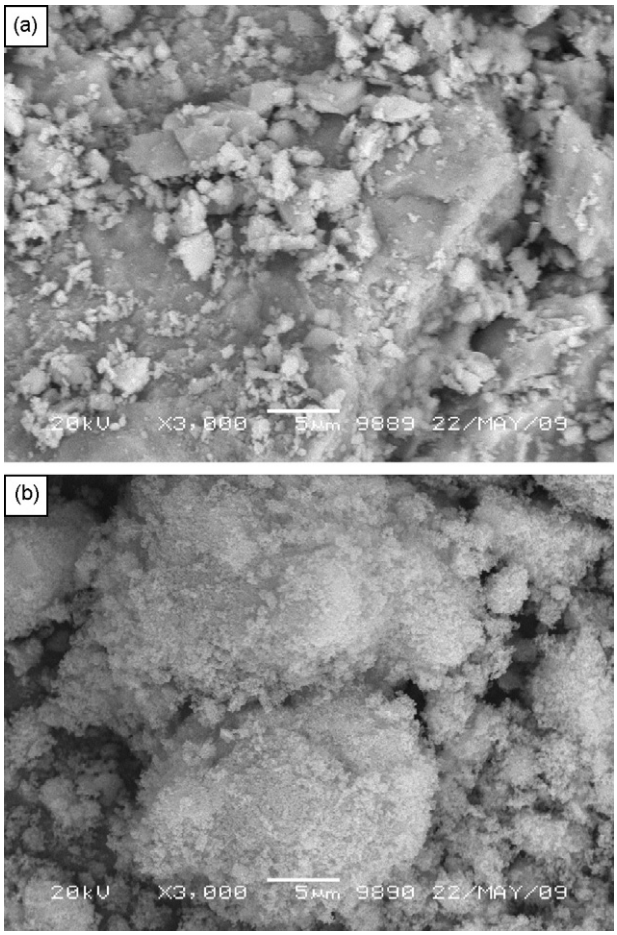


**Fig. 4.** . SEM micrographs of natural hemimorphite (a) and synthetic compound (b).

### 3.2. Thermal analysis

The results of TGA/DTA analysis of natural hemimorphite and synthetic compound are shown in Fig. 5. In the TGA curves, mass loss of both natural hemimorphite and synthetic compound starts at the beginning of the measurement due to the removal of adsorbed water. The DTG curves of natural hemimorphite and synthetic compound show some differences in the dehydration process. For the natural hemimorphite, the crystallization water is continuously lost between 364 and 581 °C. Then the structural water is lost at 685 °C. For the synthetic compound, there is an obvious evidence of the removal of absorbed water. The crystallization water is lost at lower temperature of 189 °C. And it takes two steps for the loss of structural water. The absorbed, crystallization and structural water evaporates before 700 °C with mass losses of 8.6% and 9.8% for the two samples, respectively. The theoretical mass loss can be calculated according to the equation

$$Zn_4Si_2O_7(OH)_2{\cdot}H_2O \rightarrow 2Zn_2SiO_4 + 2H_2O$$

which is 7.5%. There is no mass loss after the formation of $Zn_2SiO_4$.

A typical DTA curve of natural hemimorphite is presented in Fig. 5a, which agrees well with Liu et al.'s study [15]. A very weak endothermic peak emerges at 521 °C, which represents the loss of crystallization water. Then a strong endothermic peak ascribed to the loss of structural water to form β-$Zn_2SiO_4$ appears at 689 °C. At 900 °C, the transformation of β-$Zn_2SiO_4$ to willemite begins with an exothermic peak. Moreover, since synthetic compound is relatively poorly crystallized, the grain could be rearranged more perfectly

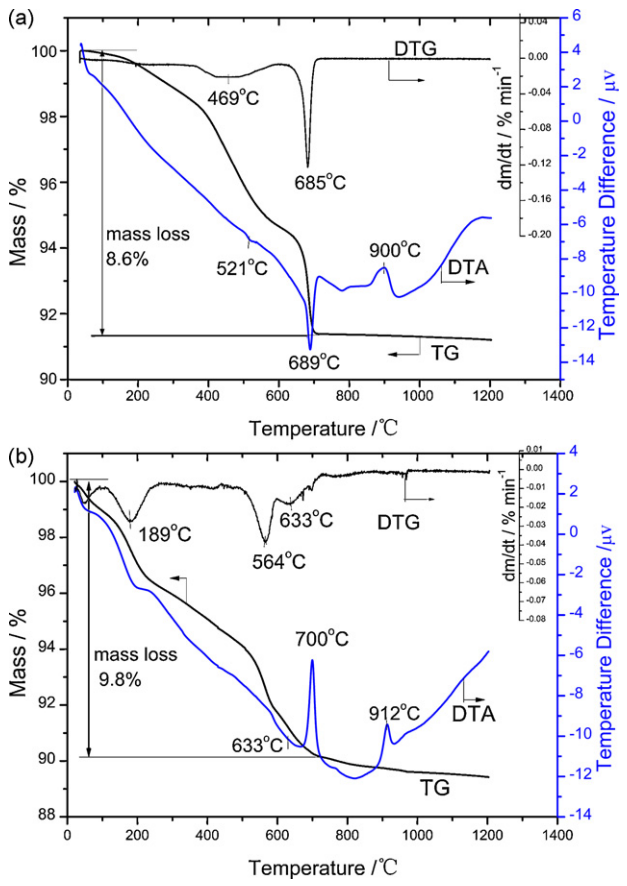


**Fig. 5.** TGA/DTA curves of natural hemimorphite (a) and synthetic compound (b).

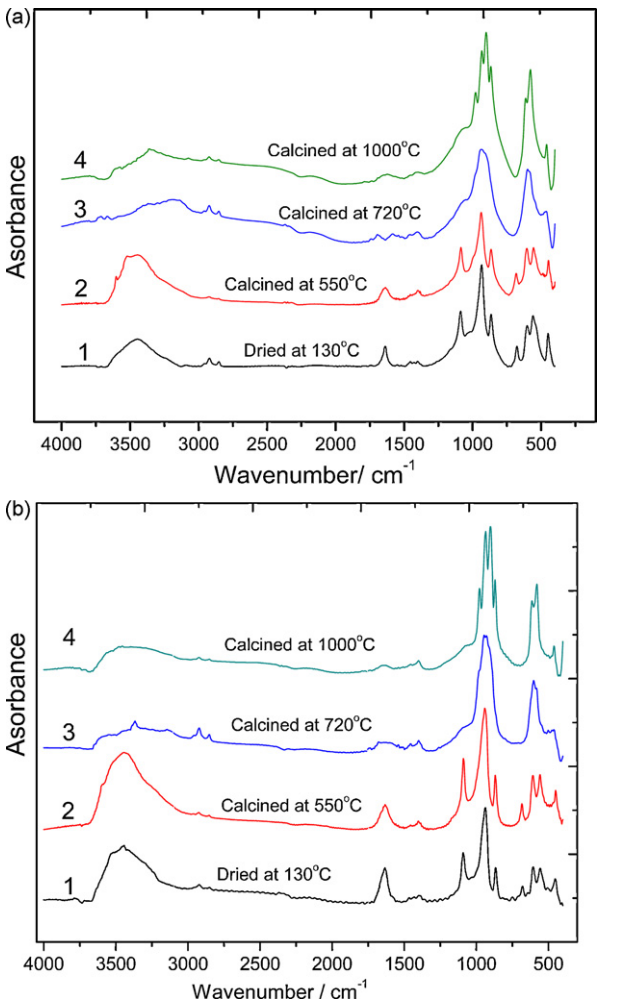


**Fig. 6.** IR spectra of natural hemimorphite (a) and synthetic compound (b) calcined at different temperature.

during or after dehydration. Therefore, a relatively wide endothermic peak due to the loss of structural water is found at 633 °C. Then a phase change with an intense exothermic peak at 700 °C happens to form a more stable phase of β-$Zn_2SiO_4$. Further phase transformation is identified at 912 °C, which is also different from the natural hemimorphite.

### 3.3. Characteristics of the calcined hemimorphite

Based on the TGA/DTA analysis of the natural hemimorphite and synthetic compound, the samples were calcined at 550 °C, 720 °C and 1000 °C, respectively. The XRD patterns of the calcined natural hemimorphite and synthetic compound are given in Figs. 2 and 3, respectively. It shows that the natural hemimorphite displays similar calcination behavior with the synthetic compound. After calcination at 550 °C, both samples are identified as dehydrated hemimorphite (JCPDS card, No. 87-1834). Comparing with the XRD patterns of curves 1 in Figs. 2 and 3, there is little change on the main peaks but a slight shrinkage of the grain size is observed (Figs. 2 and 3, curve 2). Taylor [7] studied the dehydration of hemimorphite and concluded that hemimorphite losses crystallization water and converts to β-$Zn_2SiO_4$ after calcination at 720 °C. Our study (Figs. 2 and 3, curve 3) verifies the results of Taylor's. However, the XRD pattern of β-$Zn_2SiO_4$ cannot be identified by the newest JCPDS card. Liu et al. [15] inferred it to zinc olivine, which displays as a transient phase and exists only at about 700 °C. All the samples gradually turn to willemite of hexagonal structure with nearly perfect crystallization when calcined at 1000 °C (Figs. 2 and 3, curve 4).

The infrared spectra of natural hemimorphite and synthetic compound also exhibit little difference after calcination as shown in

**Table 2**
Assignment of the bands in the IR spectra of natural hemimorphite and synthetic compound.

| Temperature | $\nu_{as}$(Si–$O_b$–Si) | | $\nu$(Si–$O_{nb}$) | | $\nu_{as}$(Si–$O_3$) | $\nu_s$(Si–$O_b$–Si) | $\delta$(Si–$O_b$–Si) | $\delta$(Si–$O_b$–Si) | $\delta$(Si–$O_b$–Si) |
|---|---|---|---|---|---|---|---|---|---|
| *Natural hemimorphite* | | | | | | | | | |
| 130 °C | 1087 | | 934 | | 865 | 677 | 600 | 559 | 449 |
| 550 °C | 1085 | | 937 | | 865 | 682 | 604 | 556 | 446 |
| 720 °C | | | 940 | | | | 601 | | 461 |
| 1000 °C | | 977 | 931 | 901 | 869 | | 614 | 577 | 460 |
| *Synthetic compound* | | | | | | | | | |
| 130 °C | 1091 | | 942 | | 867 | 679 | 607 | 557 | 452 |
| 550 °C | 1089 | | 941 | | 868 | 684 | 608 | 558 | 450 |
| 720 °C | | | 940 | | | | 602 | | 460 |
| 1000 °C | | 977 | 934 | 901 | 870 | | 616 | 578 | 460 |

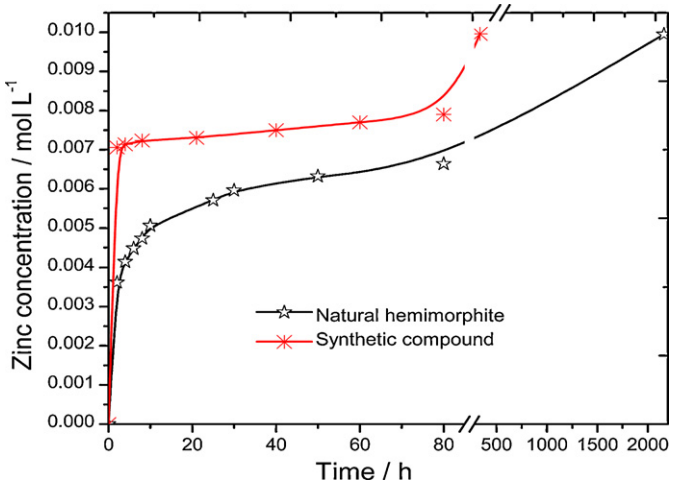


**Fig. 7.** Dissolution of Zn from natural hemimorphite and synthetic compound (solid/liquid ratio 4 g/200 ml, 1 mol/l $NH_3$ and 2 mol/l $NH_4Cl$).

Fig. 6 and Table 2. According to the literature [16], the bands of O–H bond ranging from 3600–3000 $cm^{-1}$ in the IR spectra of hemimorphite (Fig. 6, curves 1 and 2) are attributed to the $\nu$(OH) vibrations, and the medium band at 1650–1600 $cm^{-1}$ is the bending mode of $H_2O$. Bands attributed to the OH vibration for the natural hemimorphite and synthetic compound disappear after calcination at 720 °C.

The band at 1087 $cm^{-1}$ (Fig. 6, curves 1 and 2) refers to the bridge oxygen of the $Si_2O_7$ units. Its wavenumber (1087 $cm^{-1}$) as a function of the Si–$O_b$ bond length (1.6212–1.6413 Å) adjusted to Si–$O_b$–Si bond angle of 133 [17], fits well in the series of sorosilicates [18]. Meanwhile, the strong band at 677 $cm^{-1}$ is assigned to $\nu_s$(Si–$O_b$–Si) vibration. It is considered that the band at 677 $cm^{-1}$ is the one to differentiate between $Si_2O_7$ and $SiO_4$ groups as well as the band at 1087 $cm^{-1}$ by Wen et al. [19]. When samples were calcined at 720 °C, the band at 677 $cm^{-1}$ disappears in the IR spectra of natural and synthetic samples (Fig. 6, curve 3). The bands of all the samples degenerate and exhibit only three after calcination at 720 °C (Fig. 6, curve 3), since the $SiO_4$ group of the metastable zinc olivine is infrared inactive. After calcination at 1000 °C, willemite shows four bands (977, 931, 901 and 901 $cm^{-1}$; Fig. 6, curve 4 and

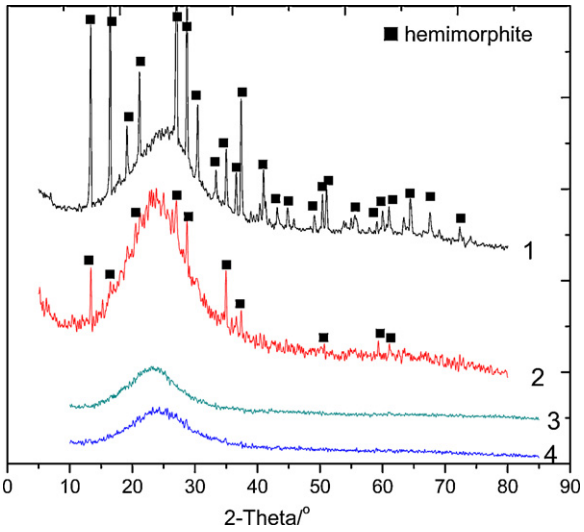


**Fig. 8.** XRD patterns of dissolution residues: (1) partial dissolution of natural hemimorphite; (2) partial dissolution of synthetic compound; (3) dissolution of natural hemimorphite; (4) dissolution of synthetic compound.

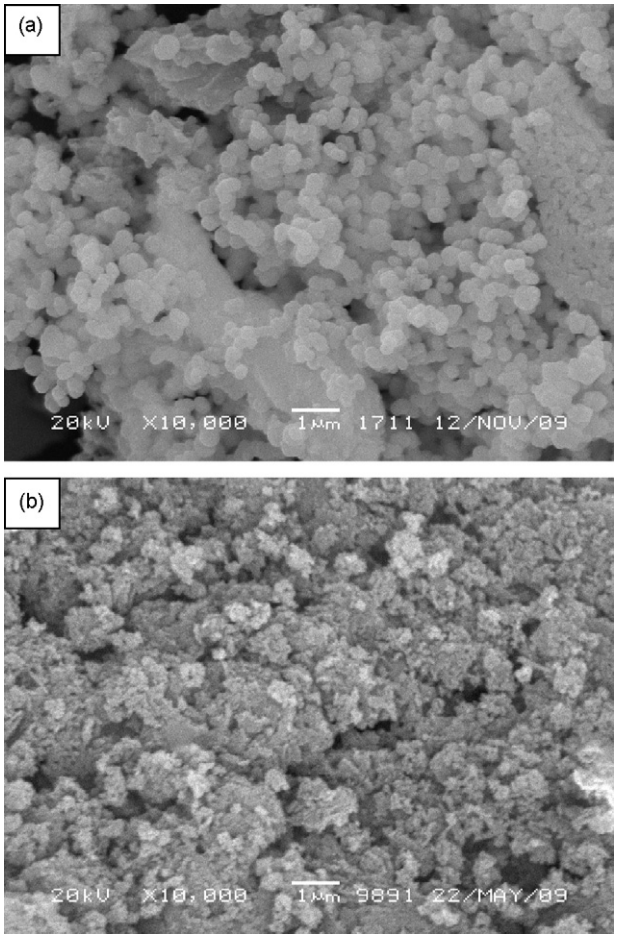


**Fig. 9.** SEM of dissolution residues: (a) natural hemimorphite; (b) synthetic compound.

Table 2) in the IR spectra ranging at 850–1000 $cm^{-1}$. Moreover, the bands at 614, 577 and 460 $cm^{-1}$ (as shown in Table 2) display a little displacement from the uncalcined samples because the structure of $SiO_4$ is different.

On the other hand, the wavenumbers of synthetic compound (1091 $cm^{-1}$ and 679 $cm^{-1}$) are higher than those of natural hemimorphite (1087 $cm^{-1}$ and 677 $cm^{-1}$), from which it could be drawn that the Si–$O_b$–Si angle of synthetic compound is larger than 133° according to Wen et al. [19]. Farmer [18] showed that there was a correction between the wavenumber of the O–Si–O antisymmetric stretching vibration and the O–Si–O bond length, from which it could be induced that the higher wavenumbers at 1091 $cm^{-1}$ and 679 $cm^{-1}$ would lead to the relative irregular crystal growth and different morphology from the natural hemimorphite.

### *3.4. Dissolution behavior of natural hemimorphite and synthetic compound*

The dissolution behavior of natural hemimorphite and synthetic compound with time was investigated. The results are given in Fig. 7, where it can be seen that zinc concentration in solution increases with the dissolution time. The dissolution rate of synthetic compound is faster than that of natural hemimorphite at the initial dissolution stage in the ammonia–ammonium chloride solution, and it would take about two weeks to get to equilibrium. By contrast, the natural hemimorphite dissolves slowly in the first 2 h, and it would take three months to get to equilibrium with a zinc concentration of 0.01 mol $L^{-1}$. Therefore, the synthetic compound reaches the dissolution equilibrium more quickly.

### 3.5. Residues analysis

Characterization of the solid residues after dissolution and partial dissolution of the natural hemimorphite and synthetic compound was done by XRD and SEM/EDS analysis. The residues from natural and synthetic samples after partial dissolution (Fig. 8, curves 1 and 2, respectively) identified by XRD are hemimorphite and an amorphous substance which is silica by EDS analysis. After complete dissolution, the hemimorphite phase in the residue of both natural and synthetic samples disappeared and only silica remained (Fig. 8, curves 3 and 4, respectively).

Fig. 9 shows the SEM micrographs of the residues of natural hemimorphite and synthetic compound after complete dissolution in ammonia–ammonium chloride solutions. The residue of natural hemimorphite appears spherical and aggregative, while that of synthetic compound seems to be irregular. The results of EDS analysis indicate that the composition of both residues is in good agreement: O 42.72% and Si 55.85% in Fig. 9a, O 42.01% and Si 56.85% in Fig. 9b, respectively. That is, the final states after complete dissolution of synthetic compound and natural hemimorphite are the same.

## 4. Conclusions

Synthetic compound, prepared by homogeneous deposition precipitation method, was identified to have the same structure as natural hemimorphite. But it is looser and more poorly crystallized.

Based on the results of TGA/DTA, IR and XRD analysis, it is found that natural hemimorphite and synthetic compound lose the crystallization water with a slight shrinkage for the grains at 469 and 189 °C, and lose the structural water at 700 and 633 °C, respectively. The poor crystallization of synthetic compound leads to the structural reorganization to form β-$Zn_2SiO_4$ with an intense exothermic peak at 700 °C.

The dissolution of synthetic compound reaches the equilibrium more quickly. The residue composition after complete dissolution of the synthetic compound is in good agreement with that of natural hemimorphite.

In conclusion, the synthetic compound shows some difference in dissolution kinetics from natural hemimorphite due to the difference in crystallinity. But the final states of natural hemimorphite and synthetic compound are the same after complete dissolution. Therefore, it is reliable to study the thermodynamics of hemimorphite by using the synthetic compound, which may also be applicable to other similar minerals.

## Acknowledgements

This work was financially supported by the National Basic Research Program of China (No. 2007CB613601). We thank Professor Pingmin Zhang for his critical comments, and we gratefully acknowledge many helpful comments and suggestions from anonymous reviewers.

## References

[1] T. Ito, J. West, The structure of hemimorphite, Z. Kristallogr. 83 (1932) 1–8.
[2] G. Bahclay, E. Cox, The structure of hemimorphite, Z. Kristallogr. 113 (1960) 23–29.
[3] W.W. Mcdonald, D.J.W. Cruickshank, Refinement of the structure of hemimorphite, Z. Kristallogr. 124 (1967) 180–191.
[4] R.J. Hill, G.V. Gibbs, J.R. Craig, A neutron diffraction study of hemimorphite, Z. Kristallogr. 146 (1977) 241–259.
[5] E. Libowitzky, A. Schultz, D. Young, The low-temperature structure and phase transition of hemimorphite, $Zn_4Si_2O_7(OH)_2{\cdot}H_2O$, Z. Kristallogr. 213 (12) (1998) 659–668.
[6] G.T. Faust, Thermal analysis and X-ray studies of sauconite and some zinc minerals of the same paragenetic association, Am. Mineral. 36 (1951) 795–822.
[7] H.F.W. Taylor, The dehydration of hemimorphite, Am. Mineral. 47 (1962) 932–944.
[8] D.M. Roy, F.A. Mumpton, Stability of minerals in the system $ZnO–SiO_2–H_2O$, Econ. Geol. 51 (1956) 432–443.
[9] J. Pomjaturad, C. Rattanakawin, N. Sriprang, Effects of additives in froth flotation of silicate zinc ore; a study by zeta potential measurement and infrared spectroscopy, Chiang Mai J. Sci. 34 (2) (2007) 191–200.
[10] C. Pereira, A. Peres, Reagents in calamine zinc ores flotation, Miner. Eng. 18 (2) (2005) 275–277.
[11] T.G. Harvey, The hydrometallurgical extraction of zinc by ammonium carbonate: a review of the Schnabel process, Miner. Process. Extr. Metall. Rev. 27 (4) (2006) 231–279.
[12] J. Frenay, Leaching of oxidized zinc ores in various media, Hydrometallurgy 15 (2) (1985) 243–253.
[13] Y. Liu, J. Deng, Q. Wang, Crystal Chemistry, Color genesis of the hemimorphite from Jinding Pb–Zn deposit, Yunnan Province, Geol. J. China Univ. 11 (3) (2005) 434–441.
[14] T. Yurieva, G. Kustova, T. Minyukova, Non-hydrothermal synthesis of copper-, zinc- and copper–zinc hydrosilicates, Mater. Res. Innov. 5 (1) (2001) 3–11.
[15] Y. Liu, J. Deng, L.Q. Yang, The dehydration of hemimorphite, Acta Petrol. Sin. 21 (3) (2005) 993–998.
[16] R.L. Frost, J.M. Bouzaid, B.J. Reddy, Vibrational spectroscopy of the sorosilicate mineral hemimorphite $Zn_4(OH)_2Si_2O_7{\cdot}H_2O$, Polyhedron 26 (2007) 2405–2412.
[17] W. Mcdonald, Refinement of the structure of hemimorphite, J. Chem. Soc. 5486 (1961) 5504.
[18] V.C. Farmer, The Infrared Spectra of Minerals, Science Press, Beijing, 1982.
[19] L. Wen, W. Liang, Z. Zhang, The Infrared Spectroscopy of Minerals, Chongqing University Press, Chongqing, 1988.